Chemical Science

EDGE ARTICLE

Check for updates

All publication charges for this article have been paid for by the Royal Society of Chemistry

Precipitation-free high-affinity multivalent binding by inline lectin ligands†

Philipp Rohse, Sabrina Weickert, Malte Drescher [ID] and Valentin Wittmann [ID] *

Multivalent ligand–protein interactions are a key concept in biology mediating, for example, signalling and adhesion. Multivalent ligands often have tremendously increased binding affinities. However, they also can cause crosslinking of receptor molecules leading to precipitation of ligand–receptor complexes. Plaque formation due to precipitation is a known characteristic of numerous fatal diseases limiting a potential medical application of multivalent ligands with a precipitating binding mode. Here, we present a new design of high-potency multivalent ligands featuring an inline arrangement of ligand epitopes with exceptionally high binding affinities in the low nanomolar range. At the same time, we show with a multi-methodological approach that precipitation of the receptor is prevented. We distinguish distinct binding modes of the ligands, in particular we elucidate a unique chelating binding mode, where four receptor binding sites are simultaneously bridged by one multivalent ligand molecule. The new design concept of inline multivalent ligands, which we established for the well-investigated model lectin wheat germ agglutinin, has great potential for the development of high-potency multivalent inhibitors as future therapeutics.

Introduction

Multivalency can drastically enhance the binding affinity between interacting species and it is a common concept used in nature.[1] Accordingly, numerous artificial multivalent ligands have been designed to interfere with natural systems. Many of these ligands have tremendously high binding affinities, but multivalent binding often results in crosslinking of the receptors. This becomes critical when receptor–ligand complexes precipitate. Plaque formation due to precipitation of proteins is known to result in numerous fatal diseases such as amyloidosis. Here, we present a solution to the problem of receptor precipitation in multivalent systems that is based on a conceptionally new design of the multivalent ligand.

A prime example for low affinity interactions that are enhanced by multivalent presentation to become physiologically relevant is the recognition of carbohydrates by lectins. Lectins participate in many important processes,[1,2] such as cell–cell, cell–pathogen, and cell–toxin interactions, for example during bacterial or viral infection, making lectins a potential target for future therapeutics.[3]

In the past, many different multivalent lectin ligands have been developed.[1,4] Typically, a scaffold is used to which mono- or oligosaccharides are attached *via* a suitable linker. Fig. 1

schematically shows different architectures that have been applied. Examples are: (A) ligands that have a central small core structure,[5] (B) ligands based on cyclic scaffolds such as cyclic peptides,[6] calixarenes[7] or cyclodextrins,[8] (C) dendrimers,[9] and (D) glycopolymers.[10] Ligands of type (E) are based on DNA or PNA[11] which allows to create rigid scaffolds with defined distances between the carbohydrate residues. (F) is a specific example where the lectin subunit of cholera toxin is modified with carbohydrates and acts as an inhibitor of native cholera toxin.[12] Example (G) illustrates ligands based on nanomaterials such as nanoparticles,[13] quantum dots,[14] carbon nanotubes,[15] or
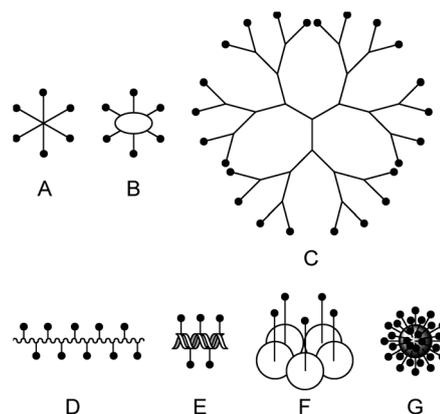

Fig. 1 Scaffolds for multivalent lectin ligands: (A) central core, (B) cyclic core, (C) dendrimer, (D) polymer, (E) DNA based, (F) protein scaffold, (G) nanomaterial.

University of Konstanz, Department of Chemistry and Konstanz Research School Chemical Biology (KoRS-CB), Universitätsstraße 10, 78457 Konstanz, Germany. E-mail: mail@valentin-wittmann.de

† Electronic supplementary information (ESI) available. See DOI: 10.1039/d0sc01744b

fullerenes.[16] For some multivalent ligands structural information on the binding mode has been obtained by X-ray crystallography.[5c,17] In many cases tremendously increased binding affinities compared to the monovalent systems have been achieved.[1,4a–c,e,18]

High binding affinities, however, are often associated with crosslinking leading to precipitation of receptor–ligand complexes[17b,c,19] thus limiting a potential medical application of a multivalent ligand. Precipitation of proteins is a hallmark of severe diseases such as Alzheimer's, Parkinson's and sickle cell disease to mention a few.[20] Hence, there is an urgent need for multivalent ligands, designed to bind with high affinity but without precipitation. Here, we present such multivalent ligands that bind to the model lectin wheat germ agglutinin (WGA) with exceptionally high binding affinities without any concomitant precipitation. By combining several analytical techniques including distance measurements by electron paramagnetic resonance (EPR) spectroscopy, we were able to obtain detailed information on the ligand binding mode.

WGA is a plant lectin isolated from *Triticum vulgaris* that has been studied extensively in the past.[21] The protein forms a stable homodimer at neutral pH exhibiting eight binding sites at the interface of the two monomers each of which is specific to *N*-acetylglucosamine (GlcNAc) and its oligomers.[17d,22] They are classified into primary binding sites with higher affinity and secondary binding sites that could be identified by X-ray crystallography but are reported to bind only weakly in solution.[23] Many multivalent ligands for WGA based on different scaffolds have been developed in the past including polymers,[24] dendrimers,[9b,25] cyclodextrins,[26] calixarenes,[7a] small glycoclusters,[6b,27] octasilsesquioxanes,[28] and quantum dots.[14] The ligands with the highest affinities reported so far are cyclic peptides presented by Fiore *et al.*[6b] and our group,[19d] octasilsesquioxanes by Lo Conte *et al.*,[28] and glycodendrimers by Ghirardello *et al.*[25c] In these examples precipitation has been observed[6b,19d] or is expected to occur.[25c,28]

Here, we present an approach, that enables high-affinity binding to WGA without precipitation. The ligand design is based on a recently solved crystal structure of WGA in complex with a divalent ligand,[17d] which showed a chelating binding mode of the ligand bridging pairs of adjacent primary WGA binding sites (Fig. 2A). From this structure it became obvious that the 6-hydroxy groups of the GlcNAc residues point away from the protein, thus offering the opportunity to link two divalent ligands in a linear fashion (Fig. 2B). In earlier studies we already used this position to link a nitroxide spin label to GlcNAc without loss of affinity.[27c] The carbohydrates are now arranged inline with the inner two GlcNAc residues being integrated into the ligand backbone, an architecture which we term inline lectin ligands (iLecs). The design is especially efficient in terms of molecular size because the carbohydrates are directly attached to each other without the need for a central scaffold. With optimized linkers, the central carbohydrate moieties are held in the binding site by two linkers leaving them less mobility to dissociate once the ligand has bound to the protein. This ligand design leads to high affinity and a defined binding mode without precipitating the protein.
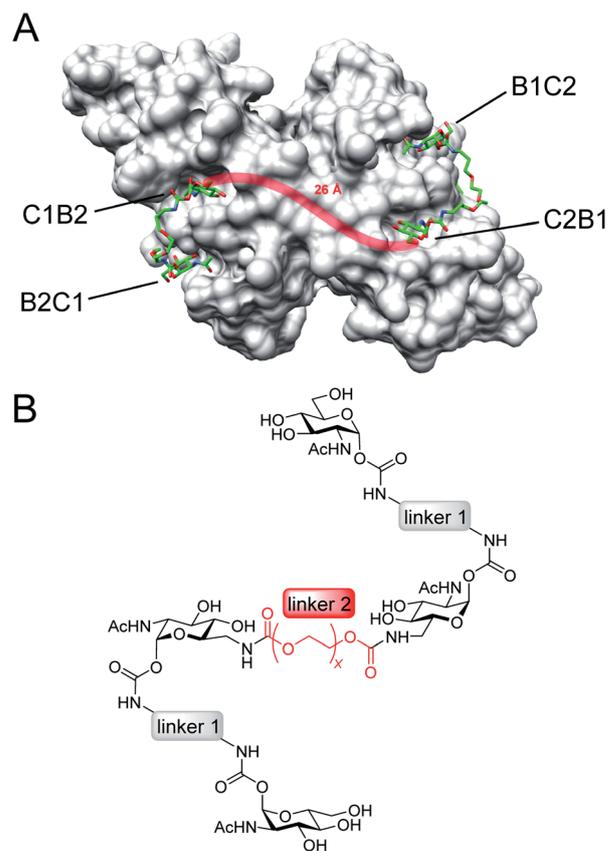

Fig. 2 (A) Crystal structure of the WGA dimer (grey, surface representation) in complex with divalent ligands (green) bridging pairs of primary binding sites named B1C2, C2B1, C1B2, and B2C1. A linker connecting two divalent ligands is sketched as red line. (B) Inline lectin ligand design.

Results and discussion

Optimization of linker 1

The design of the iLecs was carried out in two steps. Firstly, we optimized the length of linker 1 by investigating various divalent ligands. Secondly, the connection of two divalent ligands (linker 2) was addressed. To find the best linker 1 to bridge adjacent binding sites we synthesized the series of divalent ligands **1–5** (Scheme 1A) differing in the length of linker 1. Known carbonate **6** (ref. 17d and 29) was coupled to different diamines (Scheme 1B) that were derived from the corresponding diols. The resulting compounds were then *O*-deacetylated yielding divalent ligands **1–5** in up to 84% yield over two steps. Compounds **2** and **3** have already been described before.[17d]

Binding of the divalent ligands to WGA was investigated by isothermal titration calorimetry (ITC). ITC is a widely used method that provides full thermodynamic characterization and the stoichiometry of a binding event. It has been used extensively for studying carbohydrate–lectin interactions[30] and has also been used to analyze interactions of WGA with multivalent ligands.[6b,19d] The results from the ITC measurements are summarized in Table S1 (see ESI†).
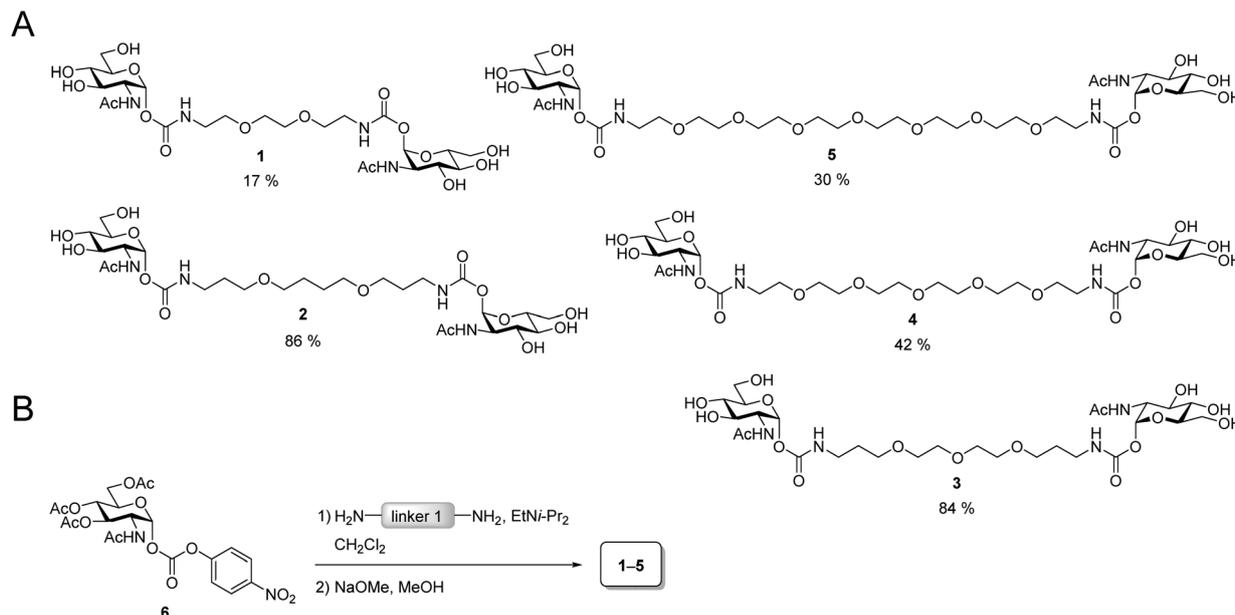
Scheme 1 (A) Divalent ligands **1–5**. (B) Synthesis of **1–5**.

The linker length has a strong impact on the binding affinity. Compound **3** has the highest binding affinity with a K_d value of 102 nM corresponding to a relative binding affinity β_{K_d} of 17 940 relative to GlcNAc. Both with increasing as well as decreasing length of linker 1, the binding affinity drops to a K_d of 730 nM for ligand **5** with the longest linker 1 and to 1.92 μM for ligand **1** which has the shortest linker 1 in the series. The stoichiometry for all ligands is approximately two ligands binding to one WGA dimer or somewhat lower. This suggests a chelating binding mode with only the primary binding sites being occupied which is in line with the results obtained previously for divalent peptidic ligands.[19d] During the ITC experiments, no precipitation was observed. However, to test, whether the divalent ligands form crosslinks leading to small aggregates, we performed dynamic light scattering (DLS) experiments.

DLS is a method that allows the determination of hydrodynamic radii of particles or macromolecules in solution and it was previously applied to investigate binding of multivalent ligands to WGA.[19d] For DLS experiments, WGA was incubated with the ligands in the stoichiometries determined by ITC. The resulting solutions were filtered through a 100 nm cutoff filter to remove dust and insoluble material before the measurements. Indeed, for ligands **1–5** no increase in the hydrodynamic radii compared to the protein alone was observed which confirms the absence of crosslinks between protein receptors in presence of the divalent ligands (see ESI†). In summary, ligand **3** which had also been crystallized with WGA before[17d] (Fig. 2A), is the optimal candidate for the development of high-affinity tetravalent ligands, since it features the highest binding affinity of all tested divalent ligands.

Synthesis of tetravalent iLecs

After the optimal length of linker 1 had been determined, we optimized the central linker (linker 2). We chose oligo(ethylene glycol) (OEG) as material as it is water-soluble, flexible and can be obtained in defined lengths. Although a rigid, perfectly fitting linker is expected to result in a maximal increase in binding affinity,[1,31] flexible linkers allow a perfect adaption of the attached carbohydrates to the binding sites, maximizing the binding enthalpy. In order to connect two divalent ligands generating the anticipated iLecs, linker 2 has to be long enough to bridge the 26 Å distance shown in Fig. 2A. OEG crystallizes in a 2/7 helix with an average monomer length of 2.78 Å.[32] The helical structure is also conserved in aqueous solution.[33] Taking this into consideration, 9.3 ethylene glycol monomers would be needed to span the distance. Assuming a completely stretched conformation (antiperiplanar conformation of all C–C and C–O bonds) the number of necessary monomers would be 7.2. In polymer science, the average end-to-end distance of a given polymer can be calculated as the Flory radius $R_F = bN^{3/5}$ with Kuhn length b and the number of monomers N.[34] Using a Kuhn length b of 7 Å,[35] the number of monomers N needed for an end-to-end distance of 26 Å is 8.9. Therefore, we decided to use hexa- to dodeca(ethylene glycol) as linker 2. These linkers include examples, which are too short to bridge the necessary distance even in a completely stretched conformation as well as linkers that are exceeding the necessary number of monomers.

The synthesis of the series of iLecs started with the reaction of OEGs **7–13** with p-nitrophenyl chloroformate **14** to form dicarbonates **15–21** in yields up to 68% (Scheme 2). The carbonates were then coupled to divalent compound **22** (ref. 27c) in which one of the 6-hydroxy groups is replaced with an amino group allowing the formation of carbamates. iLecs **23–29** were obtained in yields up to 80% after RP-HPLC purification.

Binding assays

The series of iLecs was investigated by ITC (Table 1). The highest binding affinity was found for ligand **29** with a K_d of
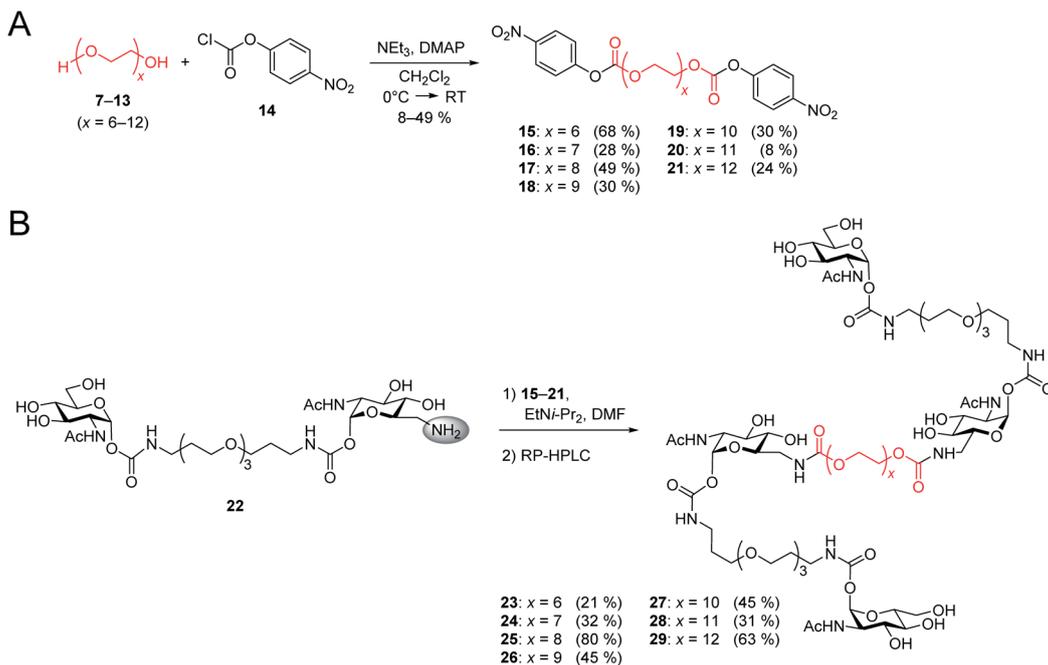
Scheme 2 (A) Synthesis of oligo(ethylene glycol) carbonates **15–21**. (B) Synthesis of tetravalent iLecs **23–29**.

Table 1 Thermodynamic binding parameters for tetravalent iLecs **23–29** binding to WGA at pH 7.0 and 298 K determined by ITC

Compound	K_d (nM)	n^a L : P	ΔH (kcal mol^{-1})	$-T\Delta S$ (kcal mol^{-1})	ΔG (kcal mol^{-1})	$\beta_{K_d}{}^c$
GlcNAc	$(1.83 \pm 0.081) \times 10^6$	4^b	-7.06 ± 0.57	3.33 ± 0.61	-3.73 ± 0.03	1
23 ($x = 6$)	3.8 ± 1.8	0.98 ± 0.02	-33.9 ± 1.5	22.2 ± 1.9	-11.6 ± 0.3	482 000
24 ($x = 7$)	4.5 ± 0.8	0.95 ± 0.01	-33.0 ± 0.1	21.5 ± 0.1	-11.4 ± 0.1	407 000
25 ($x = 8$)	4.3 ± 0.3	1.00 ± 0.02	-32.0 ± 0.4	20.6 ± 0.4	-11.5 ± 0.1	426 000
26 ($x = 9$)	5.4 ± 0.8	0.96 ± 0.05	-33.5 ± 2.8	22.6 ± 2.3	-10.9 ± 0.5	389 000
27 ($x = 10$)	2.2 ± 0.4	1.03 ± 0.03	-31.1 ± 0.8	19.3 ± 0.9	-11.8 ± 0.1	832 000
28 ($x = 11$)	3.3 ± 0.2	1.01 ± 0.02	-36.8 ± 0.7	25.2 ± 0.8	-11.6 ± 0.1	555 000
29 ($x = 12$)	1.6 ± 0.5	0.90 ± 0.01	-34.4 ± 0.7	22.3 ± 0.9	-12.1 ± 0.2	1 144 000

^{a} Binding stoichiometry, L = ligand, P = protein (dimeric WGA). ^{b} Fixed during fit.[36] ^{c} Relative binding affinity.

1.6 nM. To the best of our knowledge, this is the lowest K_d value reported for oligovalent WGA ligands so far. Also the other ligands have remarkably high affinities in the low nanomolar range. It is worth mentioning that ligands **23–26** with shorter central linkers (linker 2) have somewhat lower affinities than ligands **27–29** with longer central linkers. The binding enthalpies of the iLecs are between -31.1 kcal mol^{-1} and -36.8 kcal mol^{-1}, which is about twice as high as the binding enthalpy of ligand **3** confirming that all four GlcNAc residues bind to the protein. The stoichiometry for all ligands is close to one ligand binding per protein dimer.

We also investigated the iLecs using an enzyme-linked lectin assay (ELLA). Here, the ability of a ligand to inhibit the binding of the lectin to a surface coated with a reference ligand is tested. The assay results in IC$_{50}$ values which are the concentrations at which 50% of the binding is inhibited.[27a] The resulting dose–response curves and IC$_{50}$ values are reported in Fig. S1 (see ESI†) and Table 2, respectively. The highest inhibition potency was found for ligand **28** with an IC$_{50}$ value of 6.6 nM, closely

followed by ligands **27** and **29** with IC$_{50}$ values of 6.9 and 7.4 nM, respectively. Once again, the group of ligands **23–26** with the shorter central linkers have lower affinities ranging from 15 nM for ligand **24** to 56 nM for ligand **23**.

Table 2 Absolute and relative IC$_{50}$ values of tetravalent iLecs **23–29** for inhibition of the binding of HRP-labeled WGA to covalently immobilized GlcNAc from dose–response curves shown in Fig. S1

Compound	IC$_{50}$ (nM)	$\beta_{IC_{50}}{}^a$
GlcNAc	15×10^6	1
23	56	268 000
24	15	1 000 000
25	37	405 000
26	35	429 000
27	6.9	2 174 000
28	6.6	2 273 000
29	7.4	2 027 000

^{a} Relative inhibitory potency.

The lowest K_d values accessible by ITC are in the low nanomolar range (10^{-9}–10^{-8} M).[37] This is due to the fact that high affinity requires a low protein concentration in the experiment, which leads to a low signal to noise ratio. To determine K_d values of high-affinity interactions, competitive binding experiments have been reported.[38] The protein is pre-incubated with a known ligand of lower affinity and then the high-affinity ligand is titrated into the solution. The affinity of the strong ligand is lowered by the competing ligand, allowing the investigation of ligands with a K_d value below the detection limit. Here, we performed competitive ITC experiments using GlcNAc as a competing ligand (Table 3). We employed iLecs 23 and 29, which have the shortest and the longest central linker. In addition, we investigated tetravalent glycopeptide 30, one of the best WGA ligands ($K_d = 7$ nM) previously published.[19d] The obtained K_d values are reported as apparent $K_{d,app}$ values because there is no appropriate evaluation model available for competitive ITC experiments that accounts for multivalency effects. However, since the experimental conditions for all three ligands were the same, the $K_{d,app}$ values can be compared qualitatively. Ligand 29 has the highest affinity with $K_{d,app} = 13$ nM. This affinity is 9.5-fold higher than that of iLec 23 and even 46-fold higher than that of peptide 30. These numbers illustrate the advantage of the new iLec design over conventional multivalent WGA ligands, especially under competitive binding conditions.
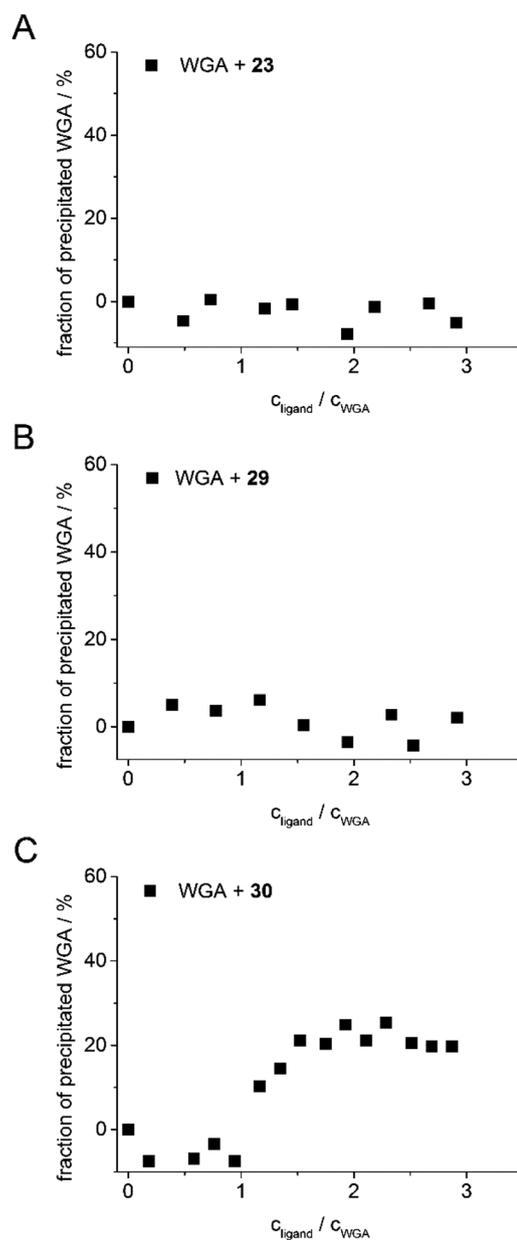
Investigation of ligand-induced protein aggregation

The aim of the new ligand design was to create a ligand that binds with high affinity without precipitating the protein. To quantify potential protein precipitation, we incubated WGA solutions (17 μM) with buffer containing 0–3 equivalents of a multivalent ligand. The solutions were then centrifuged and the protein concentration of the supernatant was determined photometrically at 280 nm. The absorption A_0 of the sample containing no ligand served as reference for 0% precipitation. With the absorption A of the samples containing ligand the precipitation was calculated according to the following formula:

$$\text{Fraction of precipitated WGA} = \frac{A_0 - A}{A_0} \times 100\%$$

As in the case of the competitive ITC measurements, iLec 23 with the shortest and 29 with the longest central linker (linker 2) were used. Remarkably, both ligands did not result in protein

Fig. 3 Precipitation profiles of WGA incubated with ligand 23 (A), with ligand 29 (B), and with ligand 30 (ref. 19d) (C). WGA solutions were incubated with varying amounts of the corresponding ligand (0–3 equiv.) for 1 h, centrifuged to remove precipitated material and the remaining protein content of the supernatant was determined photometrically at 280 nm. The fraction of precipitated WGA is plotted against the ratio of ligand to WGA.

Table 3 $K_{d,app}$ values derived from competitive ITC experiments. Ligands 23, 29, or 30 (ref. 19d) were titrated into a WGA solution (36 μM) containing GlcNAc (10 mM) as competitor

Compound	$K_{d,app}$ [nM]	$\beta_{K_{d,app}}$[a]
30	602	1
23	124	4.8
29	13	46

[a] Relative binding affinity.

precipitation (Fig. 3A and B). In contrast, addition of tetravalent glycopeptide **30** (ref. 19*d*) induced up to 20% precipitation of WGA at ligand/WGA ratios of 1.5 and higher.

Since we did not observe any precipitation upon addition of iLecs **23** or **29** to WGA, we investigated the potential formation of soluble aggregates using DLS. In Fig. 4A the intensity distributions of the hydrodynamic radius of WGA alone and of mixtures of WGA and ligand **23** or ligand **29** are shown.

While addition of ligand **23** resulted in a significant shift of the maximum of the intensity distribution to higher radii, the maximum did not change upon addition of **29** (Fig. 4A). Fig. 4B shows the mean hydrodynamic radii of mixtures of all synthesized iLecs (**23**–**29**) with WGA and Fig. 4C the corresponding calculated molecular masses. The ligands separate in two groups. Mixing WGA with ligands **23**–**26** that have shorter central linkers resulted in complexes with increased radii that correspond to approximately twice the molecular weight (red bars) of WGA (blue bar). In contrast, complexes formed with ligands **27**–**29** (green bars) do not have a significantly increased radius compared to WGA alone. In order to get further insight into the formed complexes, we performed electron paramagnetic resonance (EPR) spectroscopy measurements of selected spin-labeled iLec derivatives.

Synthesis of spin-labeled iLec derivatives

EPR spectroscopy allows the determination of distance distributions between two spin labels using the double electron–electron resonance (DEER) technique, also called PELDOR (pulsed electron–electron double resonance).[39] The method has been proven powerful for the investigation of aggregation-prone proteins relevant in Alzheimer's and Parkinson's diseases[40] as well as in the context of multivalency. In recent publications,[27c,41] we showed that DEER spectroscopy can be employed in the targeted design of multivalent ligands and that DEER distance measurements with spin-labeled divalent ligands and WGA allow to draw conclusions on the binding mode of the ligand, including the discrimination between chelating and monovalent binding. In order to apply this technique to iLecs, we attached nitroxide spin labels to the 6-positions of the terminal carbohydrates of the ligands. From EPR distance measurements between these spin labels in iLecs bound to WGA we expected to obtain valuable information on the iLec binding mode. Exemplarily, we used ligands **23** and **29** having the shortest and longest central linker 2, respectively. The short linker 2 of ligand **23** does not allow a simultaneous binding of the ligand to four binding sites of one WGA dimer. On the other hand, ligand **29** enables such a binding mode. This should lead to distinct distance distributions for both ligands in complex with WGA.

As shown in Scheme 3, the synthesis started from mono Boc-protected diamine **31** (ref. 42) which was coupled to 6-azido GlcNAc carbonate **32** (ref. 27*c*) in a yield of 80%. *O*-deacetylation of compound **33** lead to compound **34** which was hydrogenated to give **35**. At this point, the differentiation between the two different lengths of linker 2 was made. Amine **35** was coupled to either hexa- or dodeca(ethylene glycol) carbonate **15** or **21**
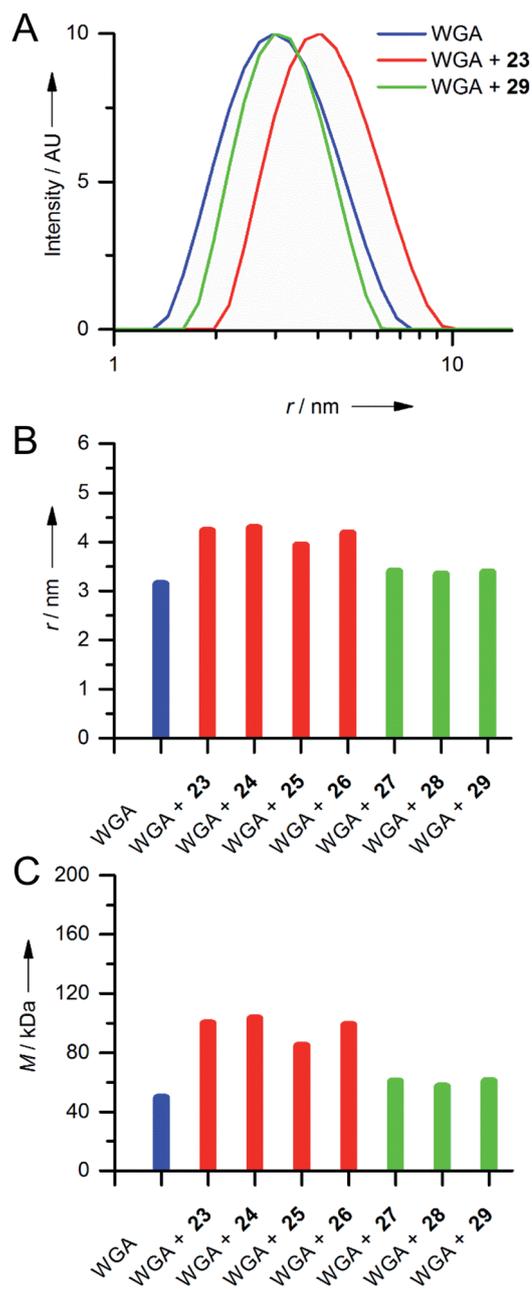

Fig. 4 Results of DLS experiments. (A) Exemplary intensity distributions of hydrodynamic radii *r* of mixtures of iLec **23** and WGA dimer at a ratio of 1 : 1 (red curve) and iLec **29** and WGA dimer at a ratio of 1 : 1 (green curve) in comparison to pure WGA (blue curve) determined by DLS after filtration through a 100 nm cutoff filter. (B) Mean hydrodynamic radii *r* (derived from intensity distributions) of species present in solutions of WGA alone (blue) and after addition of iLecs **23**–**26** (red) and **27**–**29** (green) determined by DLS after filtration through a 100 nm cutoff filter. (C) Molecular masses *M* of the species calculated from the hydrodynamic radii shown in (B) by OmniSIZE 3.0 using the built-in protein model.

followed by acetylation to give **36** or **37** in 78% yield in both cases. Removal of the Boc-protecting group and coupling of the free amine to carbonate **32** gave **38** and **39** in 83% and 90% yield, respectively. Removal of the acetyl groups led to **40** and **41**
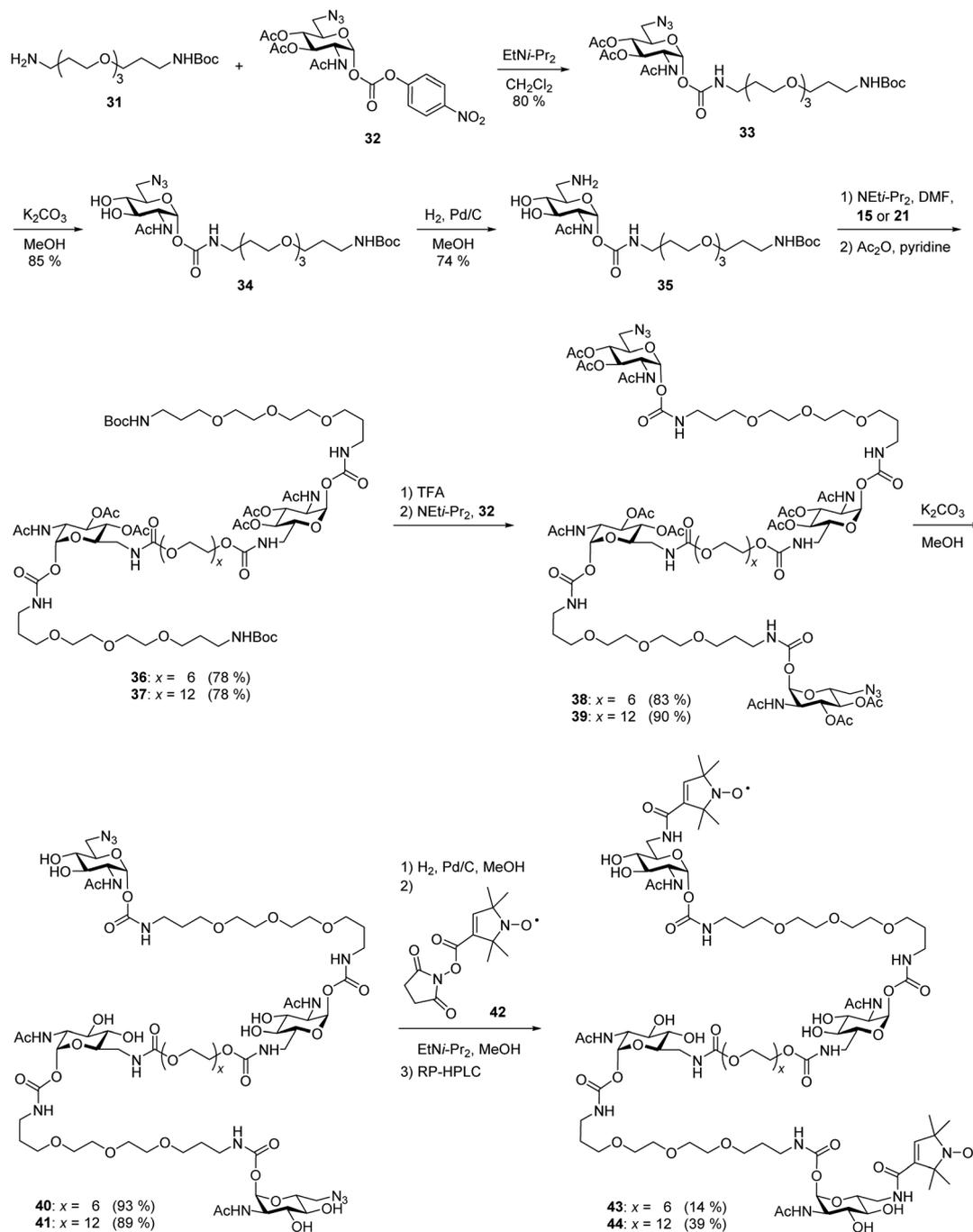
Scheme 3 Synthesis of spin–labeled iLecs **43** and **44**.

in excellent yields. Hydrogenation of the azide and subsequent coupling of the spin label using active ester **42** resulted in the spin-labeled iLecs **43** and **44** in 14% and 39% yield, respectively, after RP-HPLC purification.

EPR measurements

Spin-labeled iLecs **43** and **44** were employed in EPR distance measurements with a four-pulse DEER experiment at Q-band frequency (~34 GHz). The samples contained ligands **43** or **44** in 150 μM concentration and were prepared either in the absence or presence of 200 μM WGA dimer in aqueous solutions containing 20% (v/v) glycerol-d_8 as a cryoprotectant. The DEER experiments were performed at a temperature of 50 K after shock-freezing the samples in liquid nitrogen to trap the room temperature conformational ensemble. Distance distributions were extracted from background-corrected raw data by a model-free analysis using DEERAnalysis 2016.[43]

The distance distributions obtained with the doubly spin labeled iLecs **43** and **44** in the absence of WGA are shown in Fig. 5 (grey lines). Both ligands **43** and **44** result in rather broad

distance distributions with considerable contributions ranging from short distances of below 2 nm and up to 4 nm. The distance distributions are mainly unstructured, which suggests that the iLecs adopt a variety of conformations in solution when not bound to a protein. Upon addition of 200 μM WGA, drastic changes occur in the distance distributions of iLecs **43** (red line) and **44** (green line). As the corresponding dissociation constants are in the low nanomolar range (Table 1), both iLecs **43** and **44** bind quantitatively to WGA under the applied conditions.

For iLec **43**, that is too short to simultaneously attach to four binding sites on one WGA dimer, the distance distribution (red line) is broad, but structured and shows contributions between 2 and up to approximately 7 nm (Fig. 5). This indicates several different conformations of bound iLec **43** on WGA, which produce a variety of interspin distances. Furthermore, the largest experimentally found distances exceed the maximal possible distance between two binding sites within one WGA dimer.[17d] This suggests that spin labels located on different WGA dimers contribute to this distance distribution implying that iLec **43** crosslinks WGA dimers.

For iLec **44** the distance distribution significantly simplifies to a single narrow peak when WGA dimer is added (green line). The maximum at a distance $r = 5.1$ nm suggests that iLec **44** binds to the four primary binding sites of one WGA dimer leading to the observed end-to-end distance of the bound ligand. Comparison with the X-ray structural model confirms that the distance is in agreement with spin labeled GlcNAc moieties bound to binding sites B2C1 and B1C2 (Fig. 2A). As
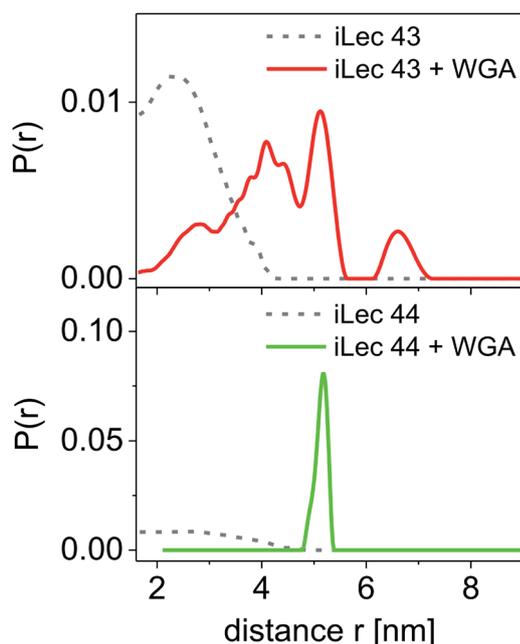
this distance exceeds the distances found in the absence of WGA, the protein obviously forces the ligand into a stretched conformation upon binding.

A modulation depth analysis of the background-corrected DEER raw data (Fig. 6) was used to further clarify the binding mode of iLecs **43** and **44**. The modulation depth of a DEER time trace can be exploited for counting the number of interacting spins per nanoobject.[44] In order to apply this method, a calibration of the modulation depth is required. Here, we used the doubly spin labeled iLecs **43** and **44** in the absence of WGA to calibrate the modulation depth to a value of 2 spin labels per nanoobject (Fig. 6, gray lines). The modulation depth of iLec **43** in the presence of WGA corresponds to 3.9 spin-labeled GlcNAc moieties per nanoobject (WGA-ligand complex). Since iLec **43** carries two spin labeled GlcNAc moieties, this is consistent with two iLec **43** molecules per WGA-ligand complex. For iLec **44**, the modulation depth translates to 2.1 spin-labeled GlcNAc moieties, which corresponds to one molecule of **44** per WGA-ligand complex.

Discussion of binding modes

The combined evidence from ITC, precipitation assays, DLS, and EPR experiments allows a precise description of the binding mode of the iLecs. The binding enthalpies derived from ITC measurements were approximately four times the value of the monosaccharide GlcNAc which indicates that all four carbohydrate residues of a ligand bind to protein. The stoichiometry of binding was approximately 1 for all iLecs meaning that complexes of ligand and WGA dimer with ratios of 1 : 1,

Fig. 5 Distance distributions for spin labeled ligand **43** and **44** ($c_{iLec} = 150$ μM). Distance distributions are normalized to the same area. Results for iLecs **43** and **44** with pure ligand are displayed as gray dotted lines and results obtained with 200 μM WGA are displayed as compact red and green lines for iLec **43** and **44**, respectively. All experiments were performed at Q-band frequency (∼34 GHz), $T = 50$ K, and 20% glycerol-d_8.
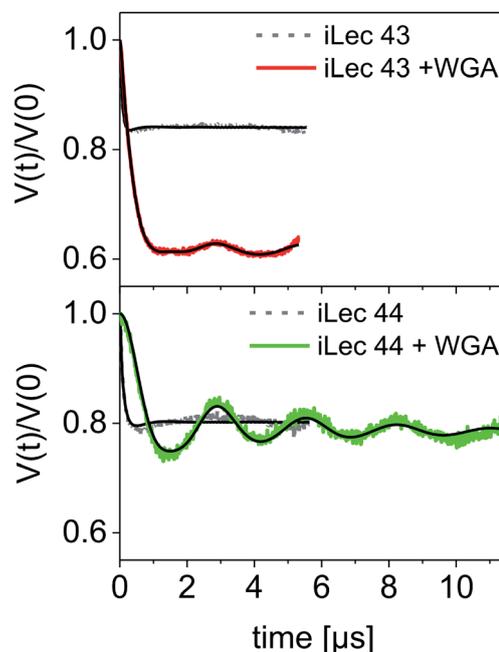

Fig. 6 DEER form factors with Tikhonov fits for ligands **43** (top) and **44** (bottom) in the absence (grey lines with black fits) and presence of WGA (red and green lines with black fits, respectively). The modulation depth of the iLec **43** experiment clearly increases upon addition of WGA to the ligand.
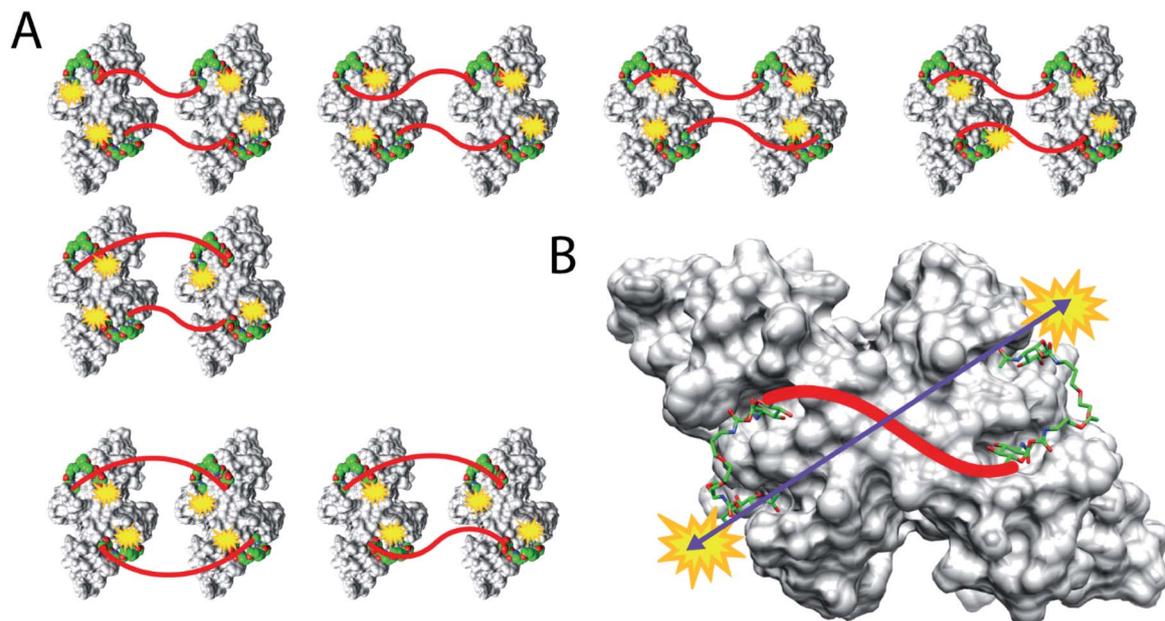
Fig. 7 Schematic representation of the binding modes of iLecs **43** and **44**. (A) Crosslinking binding of ligand **43** and the class of iLecs **23–26**. (B) Chelating binding mode for ligand **44** and the class of iLecs **27–29** resulting in a single distance between the spin labels. For clarity, linker 2 is depicted as red line.

2 : 2, *etc.* are present. The existence of big, insoluble complexes could be excluded by precipitation assays. The species that remained in solution were characterized by DLS in terms of their hydrodynamic radii. Complexes of iLecs **23–26** with shorter central linkers and WGA showed increased hydrodynamic radii of about 4 nm with a calculated molecular weight that corresponds to twice the weight of the protein alone. Complexes of iLecs **27–29** and WGA did not show an increased hydrodynamic radius. DEER experiments with spin-labeled iLec **23** (**43**) confirm the complex formation of 2 ligands with 2 WGA dimers, leading to several distances in the distance distribution and 4 spin labels per nanoobject. Spin-labeled iLec **29** (**44**) produces a single sharp distance when bound to WGA. These results allow a description of the binding mode (Fig. 7). iLecs **23–26** form complexes of two iLecs crosslinking two WGA dimers in a 2 : 2 ratio (Fig. 7A). It needs to be mentioned that several orientations of the two ligands bound to the WGA dimers are possible as it is indicated in Fig. 7A explaining the variety of interspin distances observed in the EPR experiments. iLecs **27–29** form complexes where one iLec is binding in a chelating manner, simultaneously bridging four binding sites on one WGA dimer (Fig. 7B). The distance between the terminal GlcNAc moieties is well-defined, allowing the conclusion that there is exactly one conformation the ligand adopts on the receptor surface as visualized in Fig. 7B.

Conclusion

Multivalent binding of oligo- and multivalent lectin ligands is not only a means to achieve strong binding affinities but often also results in crosslinking and precipitation of the receptor. We altered the common design strategy for multivalent lectin

ligands of attaching glycans to a central scaffold and instead developed lectin ligands that integrate the carbohydrates into the ligand backbone structure making them function as scaffold and as binding partner for the lectin. The inner carbohydrates are fixed in the ligand structure by two linkers, hampering dissociation, which is reflected by the exceptionally high binding affinities. Using ITC, precipitation assays, DLS, and EPR experiments, we characterized the binding mechanism of the ligands. With optimized linkers, multivalent ligands with exceptionally high binding affinity and a distinct binding mode are achievable that bind in a chelating manner bridging four binding sites of WGA without precipitation of the protein. We showed the importance of using a combination of different analytical techniques for the elucidation of multivalent binding to lectins. Especially EPR distance measurements proved to be a powerful tool for the analysis of binding modes. Our new concept of inline lectin ligands is a promising approach for the future development of high-affinity ligands of medically relevant lectins that bind their targets without precipitation.

Conflicts of interest

There are no conflicts to declare.

Acknowledgements

Notes and references

1 M. Mammen, S.-K. Choi and G. M. Whitesides, *Angew. Chem., Int. Ed.*, 1998, **37**, 2755–2794.

2 H. Lis and N. Sharon, *Chem. Rev.*, 1998, **98**, 637–674.

3 (*a*) A. Bernardi, J. Jimenez-Barbero, A. Casnati, C. De Castro, T. Darbre, F. Fieschi, J. Finne, H. Funken, K.-E. Jaeger, M. Lahmann, T. K. Lindhorst, M. Marradi, P. Messner, A. Molinaro, P. V. Murphy, C. Nativi, S. Oscarson, S. Penades, F. Peri, R. J. Pieters, O. Renaudet, J.-L. Reymond, B. Richichi, J. Rojo, F. Sansone, C. Schaffer, W. B. Turnbull, T. Velasco-Torrijos, S. Vidal, S. Vincent, T. Wennekes, H. Zuilhof and A. Imberty, *Chem. Soc. Rev.*, 2013, **42**, 4709–4727; (*b*) T. R. Branson and W. B. Turnbull, *Chem. Soc. Rev.*, 2013, **42**, 4613–4622; (*c*) S. Bhatia, L. C. Camacho and R. Haag, *J. Am. Chem. Soc.*, 2016, **138**, 8654–8666.

4 (*a*) J. J. Lundquist and E. J. Toone, *Chem. Rev.*, 2002, **102**, 555–578; (*b*) Y. M. Chabre and R. Roy, *Adv. Carbohydr. Chem. Biochem.*, 2010, **63**, 165–393; (*c*) C. Fasting, C. A. Schalley, M. Weber, O. Seitz, S. Hecht, B. Koksch, J. Dernedde, C. Graf, E.-W. Knapp and R. Haag, *Angew. Chem., Int. Ed.*, 2012, **51**, 10472–10498; (*d*) C. S. Mahon and D. A. Fulton, *Nat. Chem.*, 2014, **6**, 665–672; (*e*) S. Cecioni, A. Imberty and S. Vidal, *Chem. Rev.*, 2015, **115**, 525–561; (*f*) C. Müller, G. Despras and T. K. Lindhorst, *Chem. Soc. Rev.*, 2016, **45**, 3275–3302; (*g*) C. Ortiz Mellet, J.-F. Nierengarten and J. M. García Fernández, *J. Mater. Chem. B*, 2017, **5**, 6428–6436.

5 (*a*) P. Langer, S. J. Ince and S. V. Ley, *J. Chem. Soc., Perkin Trans. 1*, 1998, 3913–3916; (*b*) M. Dubber and T. K. Lindhorst, *Carbohydr. Res.*, 1998, **310**, 35–41; (*c*) P. I. Kitov, J. M. Sadowska, G. Mulvery, G. D. Armstrong, H. Ling, N. S. Pannu, R. J. Read and D. R. Bundle, *Nature*, 2000, **403**, 669–672; (*d*) C. Ligeour, O. Vidal, L. Dupin, F. Casoni, E. Gillon, A. Meyer, S. Vidal, G. Vergoten, J.-M. Lacroix, E. Souteyrand, A. Imberty, J.-J. Vasseur, Y. Chevolot and F. Morvan, *Org. Biomol. Chem.*, 2015, **13**, 8433–8444.

6 (*a*) V. Wittmann and S. Seeberger, *Angew. Chem., Int. Ed.*, 2004, **43**, 900–903; (*b*) M. Fiore, N. Berthet, A. Marra, E. Gillon, P. Dumy, A. Dondoni, A. Imberty and O. Renaudet, *Org. Biomol. Chem.*, 2013, **11**, 7113–7122.

7 (*a*) G. M. L. Consoli, F. Cunsolo, C. Geraci and V. Sgarlata, *Org. Lett.*, 2004, **6**, 4163–4166; (*b*) L. Baldini, A. Casnati, F. Sansone and R. Ungaro, *Chem. Soc. Rev.*, 2007, **36**, 254–266.

8 (*a*) I. Baussanne, J. M. Benito, C. O. Mellet, J. M. Garcia Fernandez, H. Law and J. Defaye, *Chem. Commun.*, 2000, 1489–1490; (*b*) A. Martinez, C. Ortiz Mellet and J. M. Garcia Fernandez, *Chem. Soc. Rev.*, 2013, **42**, 4746–4773.

9 (*a*) R. Roy, D. Zanini, S. J. Meunier and A. Romanowska, *J. Chem. Soc., Chem. Commun.*, 1993, 1869–1872; (*b*) N. Parera Pera, H. M. Branderhorst, R. Kooij, C. Maierhofer, M. van der Kaaden, R. M. J. Liskamp, V. Wittmann, R. Ruijtenbeek and R. J. Pieters, *ChemBioChem*, 2010, **11**, 1896–1904; (*c*)

R. U. Kadam, M. Bergmann, M. Hurley, D. Garg, M. Cacciarini, M. A. Swiderska, C. Nativi, M. Sattler, A. R. Smyth, P. Williams, M. Cámara, A. Stocker, T. Darbre and J.-L. Reymond, *Angew. Chem., Int. Ed.*, 2011, **50**, 10631–10635.

10 (*a*) A. Spaltenstein and G. M. Whitesides, *J. Am. Chem. Soc.*, 1991, **113**, 686–687; (*b*) F. D. Tropper, A. Romanowska and R. Roy, *Methods Enzymol.*, 1994, **242**, 257–271; (*c*) K. H. Mortell, R. V. Weatherman and L. L. Kiessling, *J. Am. Chem. Soc.*, 1996, **118**, 2297–2298.

11 (*a*) K. Gorska, K.-T. Huang, O. Chaloin and N. Winssinger, *Angew. Chem., Int. Ed.*, 2009, **48**, 7695–7700; (*b*) C. Scheibe, A. Bujotzek, J. Dernedde, M. Weber and O. Seitz, *Chem. Sci.*, 2011, **2**, 770–775.

12 T. R. Branson, T. E. McAllister, J. Garcia-Hartjes, M. A. Fascione, J. F. Ross, S. L. Warriner, T. Wennekes, H. Zuilhof and W. B. Turnbull, *Angew. Chem., Int. Ed.*, 2014, **53**, 8323–8327.

13 (*a*) J. M. de la Fuente, A. G. Barrientos, T. C. Rojas, J. Rojo, J. Cañada, A. Fernández and S. Penadés, *Angew. Chem., Int. Ed.*, 2001, **40**, 2257–2261; (*b*) Q. Tong, M. S. Schmidt, V. Wittmann and S. Mecking, *Biomacromolecules*, 2019, **20**, 294–304.

14 A. Robinson, J.-M. Fang, P.-T. Chou, K.-W. Liao, R.-M. Chu and S.-J. Lee, *ChemBioChem*, 2005, **6**, 1899–1905.

15 M. E. Ragoussi, S. Casado, R. Ribeiro-Viana, G. de la Torre, J. Rojo and T. Torres, *Chem. Sci.*, 2013, **4**, 4035–4041.

16 H. Kato, A. Yashiro, A. Mizuno, Y. Nishida, K. Kobayashi and H. Shinohara, *Bioorg. Med. Chem. Lett.*, 2001, **11**, 2935–2939.

17 (*a*) Y. Bourne, B. Bolgiano, D.-I. Liao, G. Strecker, P. Cantau, O. Herzberg, T. Feizi and C. Cambillau, *Nat. Struct. Biol.*, 1994, **1**, 863–870; (*b*) S. M. Dimick, S. C. Powell, S. A. McMahon, D. N. Moothoo, J. H. Naismith and E. J. Toone, *J. Am. Chem. Soc.*, 1999, **121**, 10286–10296; (*c*) E. A. Merritt, Z. Zhang, J. C. Pickens, M. Ahn, W. G. J. Hol and E. Fan, *J. Am. Chem. Soc.*, 2002, **124**, 8818–8824; (*d*) D. Schwefel, C. Maierhofer, J. G. Beck, S. Seeberger, K. Diederichs, H. M. Möller, W. Welte and V. Wittmann, *J. Am. Chem. Soc.*, 2010, **132**, 8704–8719; (*e*) S. Spjut, W. Qian, J. Bauer, R. Storm, L. Frängsmyr, T. Stehle, N. Arnberg and M. Elofsson, *Angew. Chem., Int. Ed.*, 2011, **50**, 6519–6521; (*f*) R. Visini, X. Jin, M. Bergmann, G. Michaud, F. Pertici, O. Fu, A. Pukin, T. R. Branson, D. M. E. Thies-Weesie, J. Kemmink, E. Gillon, A. Imberty, A. Stocker, T. Darbre, R. J. Pieters and J.-L. Reymond, *ACS Chem. Biol.*, 2015, **10**, 2455–2462; (*g*) V. Wittmann, *Curr. Opin. Chem. Biol.*, 2013, **17**, 982–989.

18 H. Zuilhof, *Acc. Chem. Res.*, 2016, **49**, 274–285.

19 (*a*) T. K. Dam, R. Roy, S. K. Das, S. Oscarson and C. F. Brewer, *J. Biol. Chem.*, 2000, **275**, 14223–14230; (*b*) D. Deniaud, K. Julienne and S. G. Gouin, *Org. Biomol. Chem.*, 2011, **9**, 966–979; (*c*) M. Ogata, M. Yano, S. Umemura, T. Murata, E. Y. Park, Y. Kobayashi, T. Asai, N. Oku, N. Nakamura, I. Matsuo and T. Usui, *Bioconjugate Chem.*, 2012, **23**, 97–105; (*d*) P. Rohse and V. Wittmann, *Chem.–Eur. J.*, 2016, **22**, 9724–9733.

20 (a) S. S. Wang, J. W. Wu, S. Yamamoto and H. S. Liu, *Biotechnol. J.*, 2008, **3**, 165–192; (b) R. L. Nussbaum and C. E. Ellis, *N. Engl. J. Med.*, 2003, **348**, 1356–1364; (c) D. C. Rees, T. N. Williams and M. T. Gladwin, *Lancet*, 2010, **376**, 2018–2031.

21 (a) J. P. Grivet, P. Midoux, P. Gatellier, F. Delmotte and M. Monsigny, in *Structure, Dynamics, Interactions and Evolution of Biological Macromolecules*, ed. C. Hélène, Springer, Dordrecht, 1983, pp. 329–349; (b) V. Wittmann and R. J. Pieters, *Chem. Soc. Rev.*, 2013, **42**, 4492–4503.

22 (a) C. S. Wright, *J. Mol. Biol.*, 1980, **141**, 267–291; (b) K. Harata, H. Nagahora and Y. Jigami, *Acta Crystallogr., Sect. D: Biol. Crystallogr.*, 1995, **51**, 1013–1019.

23 C. S. Wright and G. E. Kellogg, *Protein Sci.*, 1996, **5**, 1466–1476.

24 (a) S.-I. Nishimura, T. Furuike, K. Matsuoka, K. Maruyama, K. Nagata, K. Kurita, N. Nishi and S. Tokura, *Macromolecules*, 1994, **27**, 4876–4880; (b) P. Bojarova, P. Chytil, B. Mikulova, L. Bumba, R. Konefal, H. Pelantova, J. Krejzova, K. Slamova, L. Petraskova, L. Kotrchova, J. Cvacka, T. Etrych and V. Kren, *Polym. Chem.*, 2017, **8**, 2647–2658.

25 (a) D. Zanini and R. Roy, *Bioconjugate Chem.*, 1997, **8**, 187–192; (b) A. Yamada, K. Hatano, T. Koyama, K. Matsuoka, N. Takahashi, K. I. P. J. Hidari, T. Suzuki, Y. Suzuki and D. Terunuma, *Bioorg. Med. Chem.*, 2007, **15**, 1606–1614; (c) M. Ghirardello, K. Öberg, S. Staderini, O. Renaudet, N. Berthet, P. Dumy, Y. Hed, A. Marra, M. Malkoch and A. Dondoni, *J. Polym. Sci., Part A: Polym. Chem.*, 2014, **52**, 2422–2433.

26 T. Furuike, S. Aiba and S.-I. Nishimura, *Tetrahedron*, 2000, **56**, 9909–9915.

27 (a) C. Maierhofer, K. Rohmer and V. Wittmann, *Bioorg. Med. Chem.*, 2007, **15**, 7661–7676; (b) R. Masaka, M. Ogata, Y. Misawa, M. Yano, C. Hashimoto, T. Murata, H. Kawagishi and T. Usui, *Bioorg. Med. Chem.*, 2010, **18**, 621–629; (c) P. Braun, B. Nägele, V. Wittmann and M. Drescher, *Angew. Chem., Int. Ed.*, 2011, **50**, 8428–8431; (d) H. S. G. Beckmann, H. M. Möller and V. Wittmann, *Beilstein J. Org. Chem.*, 2012, **8**, 819–826.

28 M. Lo Conte, S. Staderini, A. Chambery, N. Berthet, P. Dumy, O. Renaudet, A. Marra and A. Dondoni, *Org. Biomol. Chem.*, 2012, **10**, 3269–3277.

29 T. Seitz, C. Maierhofer, D. Matzner and V. Wittmann, in *Carbohydrate Chemistry: Proven Synthetic Methods*, ed. R.

Roy and S. Vidal, CRC Press, Boca Raton, 2015, vol. 3, pp. 215–218.

30 (a) T. K. Dam and C. F. Brewer, in *Lectins*, ed. L. N. Carol, Elsevier Science B.V., Amsterdam, 2007, pp. 75–101; (b) G. Bains, R. T. Lee, Y. C. Lee and E. Freire, *Biochemistry*, 1992, **31**, 12624–12628.

31 (a) F. Pertici, N. de Mol, J. Kemmink and R. J. Pieters, *Chem.–Eur. J.*, 2013, **19**, 16923–16927; (b) V. Bandlow, S. Liese, D. Lauster, K. Ludwig, R. R. Netz, A. Herrmann and O. Seitz, *J. Am. Chem. Soc.*, 2017, **139**, 16389–16397.

32 (a) H. Tadokoro, Y. Chatani, T. Yoshihara, S. Tahara and S. Murahashi, *Makromol. Chem.*, 1964, **73**, 109–127; (b) H. Tadokoro, *Makromol. Chem.*, 1979, **2**, 155–167.

33 (a) R. Begum and H. Matsuura, *J. Chem. Soc., Faraday Trans.*, 1997, **93**, 3839–3848; (b) F. Oesterhelt, M. Rief and H. E. Gaub, *New J. Phys.*, 1999, **1**, 6; (c) M. Kobayashi and H. Sato, *Polym. Bull.*, 2008, **61**, 529–540.

34 M. Rubinstein and R. H. Colby, *Polymer Physics*, Oxford University Press, Oxford, 2003.

35 F. Kienberger, V. P. Pastushenko, G. Kada, H. J. Gruber, C. Riener, H. Schindler and P. Hinterdorfer, *Single Mol.*, 2000, **1**, 123–128.

36 W. B. Turnbull and A. H. Daranas, *J. Am. Chem. Soc.*, 2003, **125**, 14859–14866.

37 E. Freire, O. L. Mayorga and M. Straume, *Anal. Chem.*, 1990, **62**, 950A–959A.

38 B. W. Sigurskjold, *Anal. Biochem.*, 2000, **277**, 260–266.

39 (a) A. D. Milov, A. B. Ponomarev and Y. D. Tsvetkov, *Chem. Phys. Lett.*, 1984, **110**, 67–72; (b) M. Pannier, S. Veit, A. Godt, G. Jeschke and H. W. Spiess, *J. Magn. Reson.*, 2000, **213**, 316–325; (c) G. Jeschke, *Annu. Rev. Phys. Chem.*, 2012, **63**, 419–446.

40 S. Weickert, J. Cattani and M. Drescher, *Electron Paramagn. Reson.*, 2019, **26**, 1–37.

41 S. Weickert, T. Seitz, W. K. Myers, C. R. Timmel, M. Drescher and V. Wittmann, *J. Phys. Chem. Lett.*, 2018, **9**, 6131–6135.

42 T. T. Hai, D. E. Pereira, D. J. Nelson, J. Catarello and A. Srnak, *Bioconjugate Chem.*, 2000, **11**, 705–713.

43 G. Jeschke, V. Chechik, P. Ionita, A. Godt, H. Zimmermann, J. Banham, C. R. Timmel, D. Hilger and H. Jung, *Appl. Magn. Reson.*, 2006, **30**, 473–498.

44 (a) B. E. Bode, D. Margraf, J. Plackmeyer, G. Dürner, T. F. Prisner and O. Schiemann, *J. Am. Chem. Soc.*, 2007, **129**, 6736–6745; (b) D. Hilger, H. Jung, E. Padan, C. Wegener, K.-P. Vogel, H.-J. Steinhoff and G. Jeschke, *Biophys. J.*, 2005, **89**, 1328–1338.